Anomalous Electromagnetic Field Penetration in a Weyl or Dirac Semimetal

P. O. Sukhachov* and L. I. Glazman
Department of Physics, Yale University, New Haven, Connecticut 06520, USA

(Received 29 October 2021; revised 3 January 2022; accepted 8 March 2022; published 6 April 2022)

The current response to an electromagnetic field in a Weyl or Dirac semimetal becomes nonlocal due to the chiral anomaly activated by an applied static magnetic field. The nonlocality develops under the conditions of the normal skin effect and is related to the valley charge imbalance generated by the joint effect of the electric field of the impinging wave and the static magnetic field. We elucidate the signatures of this nonlocality in the transmission of electromagnetic waves. The signatures include enhancement of the transmission amplitude and its specific dependence on the wave's frequency and the static magnetic field strength.

DOI: 10.1103/PhysRevLett.128.146801

Introduction.—A salient feature of Weyl and Dirac materials is the possibility to realize the chiral anomaly due to their relativisticlike electronic spectra in the vicinity of the band-touching nodal points. As was pointed out in Ref. [1], this is an analog of the Adler-Bell-Jackiw axial anomaly in relativistic physics [2,3]. The chiral Adler-Bell-Jackiw anomaly was first observed in Weyl superfluid ^{3}He-A [4]. In the solid-state physics setting, the anomaly may lead to a negative magnetoresistance in the direction parallel to the applied magnetic field. Interest in the manifestations of the chiral anomaly in the electron transport flared up after the discovery of Weyl semimetals [5–7]. The kinetic theory of negative magnetoresistance in direct current (dc) transport was fleshed out [8], and its dependence on the electron spectra and relaxation times was elucidated. A negative magnetoresistance was indeed observed in Dirac (e.g., Na_3Bi, Cd_3As_2, and $ZrTe_5$) and Weyl (e.g., transition metal monopnictides TaAs, NbAs, TaP, and NbP) semimetals (see Refs. [9–13] for reviews on anomalous transport properties). However, it was soon realized that the observation of the negative magnetoresistivity alone is not sufficient to claim the realization of the chiral anomaly. Among the effects that can mimic the anomaly are current jetting [14,15] due to an inhomogeneous distribution of the electric current in materials with high mobility and electron scattering on long-range ionic impurities [16].

It was suggested in Ref. [17] to use frequency as an additional control "knob" to investigate the effects of the chiral anomaly while circumventing the current jetting: in the presence of a magnetic field, the anomaly results in a Drude-like contribution to the conductivity. The width of the corresponding low-frequency peak in the linear alternating current (ac) response to a spatially uniform electric field is determined by the internode relaxation rate. The latter rate is usually small compared with the intranode relaxation rate, so the anomalous conductivity peak is fairly narrow. The tendency toward peak narrowing was seen in the contactless measurements of the transmission amplitude of an electromagnetic field through a Cd_3As_2 film [18].

The electric field of the wave penetrating a material, however, is nonuniform due to the skin effect. This raises a question regarding the influence of chiral anomaly on the transmission of an electromagnetic wave across a film made of a Weyl or Dirac conductor.

We demonstrate in this Letter that an application of a magnetic field parallel to the surface of a Weyl or Dirac conductor activates the chiral anomaly and may result in a nonlocal current response to an impinging electromagnetic wave. We emphasize that this nonlocal response develops under the conditions corresponding to the normal skin effect. The latter is thought to be adequate for materials with the electron mean free path shorter than the electromagnetic field penetration depth [19]. A new element brought by the topological electronic band structure is the valley charge imbalance. It is activated via the chiral anomaly by the joint effect of the electric field of the impinging wave, active within the skin layer, and a static magnetic field. The valley charge imbalance preserves the local charge neutrality and therefore is not suppressed by screening. This property allows the imbalance to diffuse beyond the skin depth, deeper into the sample. The accompanying chiral magnetic effect [20,21] current represents the nonlocal response to the electric field of the impinging wave and facilitates its anomalous penetration, similar to a dc nonlocal transport [22–24].

The three main regimes of the current response including dc, ac local, and ac nonlocal regimes are schematically illustrated in Fig. 1. In this work, unlike the existing studies (e.g., Ref. [18]) of the chiral anomaly performed in the local regimes (see the blue dotted line in Fig. 1), we focus on the *ac nonlocal* regime with a spatial dispersion of the conductivity (see the red dotted line in Fig. 1).

 © 2022 American Physical Society

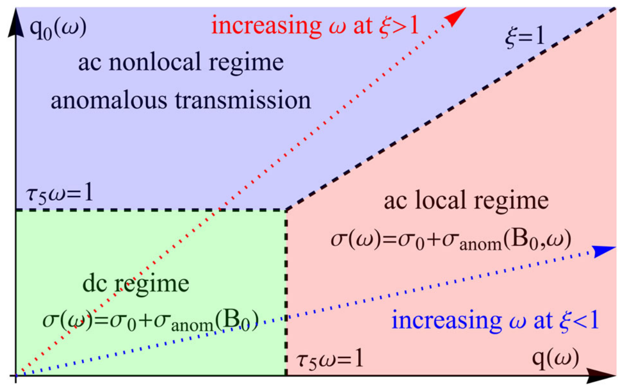

FIG. 1. The schematic representation of the current response regimes discussed in this work. Here $q_0(\omega) = 1/\delta(\omega) = \sqrt{2\pi\sigma_0\omega}/c$ is inverse of the skin depth, σ_0 is the static Drude conductivity, ω is the angular frequency of the impinging wave, $q(\omega) = \sqrt{\omega/(2D)}$ is inverse of the diffusion length, D is the diffusion coefficient, $\xi = q_0(\omega)/q(\omega) = \sqrt{4\pi\sigma_0 D}/c$ is the frequency-independent parameter quantifying the nonlocality of the response, and $1/\tau_5$ is the effective internode scattering rate. In addition, we assume a short intranode scattering time τ, i.e., $\omega\tau \ll 1$. The transmission of electromagnetic waves is described via the standard expressions for the normal skin effect [19] with conductivity modified by the chiral anomaly, $\sigma(\omega) = \sigma_0 + \sigma_{\rm anom}(B_0, \omega)$, in the dc and ac local ($\xi < 1$) regimes; see Eq. (10) for the transmitted electric field. In the ac nonlocal regime ($\xi > 1$), it is possible to achieve an enhancement of the electromagnetic wave penetration depth; see Eqs. (8) and (9).

Model and key equations.—To study the transmission of electromagnetic waves, we consider a film of a Dirac or time-reversal symmetric Weyl semimetal [25] with the thickness L along the z direction. We assume the normal incidence of the incoming ($z \leq 0$) wave with an electric field $\mathbf{E}_{\rm in}(t,z) = \mathbf{E}_{\rm in} e^{i(kz-\omega t)}$, where ω is the angular frequency and $k = \omega/c$ is the wave vector. A portion of the incoming field $\mathbf{E}_r(t,z)$ is reflected from the surface, and a portion $\mathbf{E}_{\rm out}(t,z)$ is transmitted across the film. The in-medium field $\mathbf{E}(t,z)$ satisfies the standard system of Maxwell's equations. To close it, one needs to evaluate the current density as a response to the electric field. This (generally nonlocal) linear response is controlled by the electron kinetics. In building the kinetic theory of a Weyl or Dirac semimetal, we assume that the characteristic intranode relaxation times are much shorter than the internode ones in accordance with experiments, see, e.g., Refs. [18,27]. In addition, the intranode scattering rates are assumed to be much larger than the frequency of the electromagnetic field. To activate the chiral anomaly, we include a static uniform magnetic field $\mathbf{B}_0$, which is applied parallel to the surface and is classically weak [28]. Under this condition, $\mathbf{B}_0$ does not affect the diffusive electron dynamics while introducing an anomalous term into the partial current density $\mathbf{j}_\alpha(t,z)$ produced by electrons of node α [29],

$$\mathbf{j}_\alpha(t,z) = \sigma_\alpha \mathbf{E}(t,z) - D_\alpha \boldsymbol{\nabla} N_\alpha(t,z) - \mathbf{v}_{\Omega,\alpha} N_\alpha(t,z). \tag{1}$$

Here $N_\alpha(t,z)$ is the perturbed partial (or valley) electron charge density at node α and $\mathbf{v}_{\Omega,\alpha}$ is the anomalous velocity associated with the flux χ_α of the Berry curvature; D_α and $\sigma_\alpha = e^2\nu_\alpha D_\alpha$ are the respective diffusion constant and partial electric conductivity. In terms of χ_α and the Fermi level density of states ν_α of electrons around node α, the anomalous velocity is $\mathbf{v}_{\Omega,\alpha} = \chi_\alpha e \mathbf{B}_0/(4\pi^2\hbar^2 c\nu_\alpha)$. While the first two terms in Eq. (1) correspond to the conventional intranode diffusion current, the last term describes the chiral magnetic effect current [20,21] after summing over all nodes.

The kinetic equation in the diffusive approximation is

$$\partial_t N_\alpha(t,z) + \boldsymbol{\nabla}\cdot\mathbf{j}_\alpha(t,z) = -\sum_\beta^{N_W} T_{\alpha,\beta} N_\beta(t,z) - e^2\nu_\alpha \mathbf{v}_{\Omega,\alpha}\cdot\mathbf{E}(t,z); \tag{2}$$

see the Supplemental Material [31] and, e.g., Refs. [10,22,36] for details. The terms on the left-hand side of Eq. (2) correspond to the conventional continuity equation in each of the nodes. On the right-hand side, the shorthand notation $T_{\alpha,\beta} = \delta_{\alpha,\beta}\sum_\gamma^{N_W} 1/\tau_{\alpha,\gamma} - 1/\tau_{\beta,\alpha}$ in the term responsible for the internode scattering in the relaxation time approximation was introduced. Here N_W is a number of Weyl nodes and $1/\tau_{\alpha,\beta}$ are the scattering rates between nodes α and β. Finally, the last term in Eq. (2) corresponds to the chiral anomaly. It is important to note that the total electric charge $\sum_\alpha^{N_W} N_\alpha(t,z)$ is conserved by the collision integral and the chiral anomaly. In addition, the transverse field, $\boldsymbol{\nabla}\cdot\mathbf{E}(z) = 0$, in Eq. (2) does not violate the electric charge neutrality.

Since the time dependence of fields, currents, and densities is given by the same prefactor $e^{-i\omega t}$, we combine Eqs. (1) and (2) as

$$\sum_\beta^{N_W}\left[\frac{T_{\alpha,\beta}}{D_\alpha} - 2iq_\alpha^2(\omega)\delta_{\alpha,\beta} - \delta_{\alpha,\beta}\partial_z^2\right]N_\beta(z) = -\frac{e^2\nu_\alpha}{D_\alpha}\mathbf{v}_{\Omega,\alpha}\cdot\mathbf{E}(z), \tag{3}$$

where $q_\alpha(\omega) = \sqrt{\omega/(2D_\alpha)}$ is the inverse of the diffusion length. Finally, neglecting the displacement current for $\omega \ll \sigma_0$ with $\sigma_0 = \sum_\alpha^{N_W}\sigma_\alpha$ being the static conductivity, Maxwell's equations for the transverse components of the electric field together with the equation for current [Eq. (1)] are brought to the following form:

$$[\partial_z^2 + 2iq_0^2(\omega)]\mathbf{E}(z) = \frac{4\pi i\omega}{c^2}\sum_\alpha^{N_W} \mathbf{v}_{\Omega,\alpha} N_\alpha(z), \quad (4)$$

where $q_0(\omega) = \sqrt{2\pi\sigma_0\omega}/c$ is the inverse of the skin depth.

In order to form a complete system for the transverse electric field $\mathbf{E}(z)$ and the valley charge densities $N_\alpha(z)$, Eqs. (3) and (4) should be amended with boundary conditions. We use the standard boundary conditions for electromagnetic fields, i.e., we require the continuity of the tangential component of the electric fields and their derivatives [37] at $z = 0, L$. As for the densities, we consider two types of phenomenological boundary conditions:

$$\text{(i) } N_\alpha(z=0,L) = 0 \quad \text{and} \quad \text{(ii) } \partial_z N_\alpha(z=0,L) = 0. \quad (5)$$

These two conditions correspond, respectively, to the limits of fast and no internode relaxation at the boundary.

Transmission of electromagnetic waves.—A finite anomalous velocity $\mathbf{v}_{\Omega,\alpha}$ emerging at $B_0 \neq 0$ couples the electric field $\mathbf{E}(z)$ of the wave to the diffusion of partial densities $N_\alpha(z)$. The spectrum of the diffusion length scales can be found by solving the eigenvalue problem for the coupled set of the diffusion equations; see Eq. (3) for a diffusion equation at node α. In general, the spectrum of the diffusion lengths depends on the internode relaxation rates. However, in the limit of ω being high compared with the characteristic value $1/\tau_5$ of the internode scattering rates, the diffusion equations decouple from each other, and the diffusion lengths are quantified by $1/q_\alpha(\omega)$. We note that the ratio $\xi_\alpha = q_0(\omega)/q_\alpha(\omega) = \sqrt{4\pi\sigma_0 D_\alpha}/c$ is defined solely by the material properties and is independent of ω. The anomalous penetration of the field is driven by the largest among ξ_α. Aiming at a strong anomalous effect, we assume $\xi_\alpha \gg 1$ for all α and consider films of thickness far exceeding the normal-skin penetration depth $L \gg 1/q_0(\omega)$.

It is convenient to separate the electric field into two components, $\mathbf{E}(z) = \mathbf{E}_\parallel(z) + \mathbf{E}_\perp(z)$, parallel and normal to $\mathbf{B}_0$, respectively. The anomaly affects only the former one, while $|E_\perp(z)| \propto e^{-Lq_0(\omega)}$ is independent of B_0. When evaluating $\mathbf{E}_\parallel(z)$, we focus on the most practical case of weak coupling between $\mathbf{E}_\parallel(z)$ and $N_\alpha(z)$. This allows us to solve Eqs. (3) and (4) iteratively in $\mathbf{v}_{\Omega,\alpha}$ by starting with $E_\parallel^{(0)}(z) = (1-i)(\omega/c)e^{-zq_0(\omega)}e^{izq_0(\omega)}E_{\parallel\text{in}}/q_0(\omega)$ at $L - z \gg 1/q_0(\omega)$ within the film; the corresponding outgoing field follows from the boundary conditions and reads $E_{\parallel\text{out}}^{(0)}(z=L) = 2(1-i)(\omega/c)e^{-Lq_0(\omega)}e^{iLq_0(\omega)}E_{\parallel\text{in}}/q_0(\omega)$. Being substituted into the right-hand side of Eq. (3), $E_\parallel^{(0)}(z)$ creates a source exciting valley charge density imbalance. The resulting solution $N_\alpha^{(1)}(z) \propto v_{\Omega,\alpha}$ reads [31] as

$$N_\alpha^{(1)}(z) = -i\frac{e^2\nu_\alpha v_{\Omega,\alpha}}{2q_0^2(\omega)D_\alpha}\frac{\sin[(1+i)(L-z)q_\alpha(\omega)]}{\sin[(1+i)q_\alpha(\omega)L]}E_\parallel^{(0)}(0) \quad (6)$$

for the Dirichlet boundary conditions [Eq. (5)]. In solving Eq. (3), we assumed a highly nonlocal regime, $\xi_\alpha \gg 1$, and considered $z \gg 1/q_0(\omega)$.

Lastly, we use Eq. (6) on the right-hand side of Eq. (4) to find the anomalous correction $E_\parallel^{(2)}(z) \propto v_{\Omega,\alpha}^2$ to the electric field. The solution to Eq. (4) is simplified by a slow spatial variation of the partial densities, $1/q_\alpha(\omega) = \xi_\alpha/q_0(\omega) \gg 1/q_0(\omega)$, allowing us to write

$$E_\parallel^{(2)}(z) = \frac{1}{\sigma_0}\sum_\alpha^{N_W} v_{\Omega,\alpha}\bigg[N_\alpha^{(1)}(z) - \frac{1+i}{2q_0(\omega)} \times e^{-(L-z)q_0(\omega)}e^{i(L-z)q_0(\omega)}\partial_z N_\alpha^{(1)}(z=L)\bigg]. \quad (7)$$

This form is valid for either of the two boundary conditions for $N_\alpha(z)$. The outgoing field follows from the continuity of the tangential components of the electric field, i.e., $E_{\parallel\text{out}}^{(2)}(z=L) = E_\parallel^{(2)}(z=L)$.

We consider two characteristic cases of a thick film, $L \gg 1/q_\alpha(\omega)$, and a thin film, $L \ll 1/q_\alpha(\omega)$, compared with the diffusion lengths. In the former case, the partial charge density decays exponentially with z. Using Eq. (7), we find the following transmitted electric field:

$$E_{\parallel\text{out}}(t, z=L) = 2\sqrt{\frac{\omega}{\pi\sigma_0}}\bigg[e^{-L/\delta(\omega)}\cos\left(\frac{L}{\delta(\omega)} - \frac{\pi}{4} - \omega t\right) - \sum_\alpha^{N_W}\frac{g_\alpha}{\xi_\alpha^3}\frac{B_0^2}{B_\alpha^2(\omega)}e^{-L/[\xi_\alpha\delta(\omega)]} \times \cos\left(\frac{L}{\xi_\alpha\delta(\omega)} + \frac{\pi}{4} - \omega t\right)\bigg]E_{\parallel\text{in}}, \quad (8)$$

where $g_\alpha = 1$ for $N_\alpha^{(1)}(z=0,L) = 0$ and $g_\alpha = \xi_\alpha^2$ for $\partial_z N_\alpha^{(1)}(z=0,L) = 0$, respectively. For clarity, in Eq. (8), we restored the real part for the fields, used the conventional definition for the normal-skin depth, $\delta(\omega) = c/\sqrt{2\pi\sigma_0\omega}$, and introduced the characteristic magnetic field $B_\alpha(\omega) = 4\pi\Phi_0\hbar\sqrt{\omega\nu_\alpha\sum_\beta^{N_W}\nu_\beta D_\beta}$, which depends on the electronic properties of the material and frequency. In writing $B_\alpha(\omega)$, we used the explicit expression for $\mathbf{v}_{\Omega,\alpha}$ and $\sigma_0 = e^2\sum_\alpha^{N_W}\nu_\alpha D_\alpha$ for the Drude conductivity; $\Phi_0 = \pi\hbar c/e$ is the magnetic flux quantum. While the terms in Eq. (8) representing the conventional and anomalous components of the transmitted field both decay exponentially with the film thickness, the respective penetration depths are vastly different at $\xi_\alpha \gg 1$.

In the case of a thin film, $L \ll 1/q_\alpha(\omega)$, the partial charge, which is created in the skin layer, spreads over the entire thickness of the film L due to diffusion. Substituting the proper limit of Eq. (6) that defines $N^{(1)}_\alpha(z)$ into Eq. (7), we find

$$E_{\|\mathrm{out}}(t, z=L) = 2\sqrt{\frac{\omega}{\pi\sigma_0}}\left[e^{-L/\delta(\omega)}\cos\left(\frac{L}{\delta(\omega)} - \frac{\pi}{4} - \omega t\right) - \frac{1}{2\sqrt{2}}\frac{\delta(\omega)}{L}\sum_\alpha^{N_W}\frac{g_\alpha}{\xi_\alpha^2}\frac{B_0^2}{B_\alpha^2(\omega)}\sin(\omega t)\right]E_{\|\mathrm{in}}. \tag{9}$$

As expected, the anomalous correction to the outgoing electric field (the second term) acquires a $\propto 1/L$ scaling with the film thickness. In the case of the Dirichlet boundary conditions ($g_\alpha = 1$), there is an additional small prefactor $1/\xi_\alpha^2$ that originates from the suppression of $N^{(1)}_\alpha(z)$ near the boundaries. Such suppression is absent for the Neumann boundary conditions ($g_\alpha = \xi_\alpha^2$) where a uniform partial charge density is allowed [31].

To contrast the results for the local and nonlocal regimes, we also present the transmitted field at $\xi_\alpha \ll 1$. It can be obtained by introducing the anomalous correction to the electric conductivity in the standard expression for the normal skin effect; see the Supplemental Material [31] for details. In the leading order in B_0, we have

$$E_{\|\mathrm{out}}(t, z=L) = 2\sqrt{\frac{\omega}{\pi\sigma_0}}e^{-L/\delta(\omega)}\left[\cos\left(\frac{L}{\delta(\omega)} - \frac{\pi}{4} - \omega t\right) - \frac{1}{\sqrt{2}}\frac{L}{\delta(\omega)}\sum_\alpha^{N_W}\frac{B_0^2}{B_\alpha^2(\omega)} \times \cos\left(\frac{L}{\delta(\omega)} - \omega t\right)\right]E_{\|\mathrm{in}}, \tag{10}$$

where, as in the case of the nonlocal response, we neglected the internode scattering. As one can see by comparing Eqs. (8)–(10), the scaling of the anomalous parts of the transmitted fields with frequency is qualitatively different and might be used to distinguish nonlocal and local response regimes even if material parameters are not known *a priori*. Furthermore, it is straightforward to check [31] that the amplitude of the transmitted field in the local regime always decreases with the magnetic field. On the other hand, interference between the anomalous and the regular terms in Eq. (8) or (9) may lead to an enhancement of the transmitted field at $B_0 \neq 0$.

Estimates for a model with symmetric Weyl nodes.—To provide estimates of the proposed effects, we consider a simplified model with N_W Weyl nodes forming well-separated from each other symmetric pairs. Each pair consists of nodes carrying opposite topological charges. We assume the electron dispersion around each of the nodes to be linear, with the same parameters $\nu_\alpha \to \nu$ and $D_\alpha \to D$. This allows us to introduce the node-independent electron mean free path $\ell = v_F\tau$ with the intranode relaxation time τ, and replace $\xi_\alpha \to \xi$. With these simplifications, we reformulate the condition of the normal skin effect, $\ell \ll \delta(\omega)$, as $\xi\sqrt{\omega\tau} \ll 1$. Therefore, our approximations are valid for the following double constraint on ξ: $1 \ll \xi \ll 1/\sqrt{\omega\tau}$. The lower constraint on frequency ω comes from the internode relaxation rate. In our model, the corresponding rate, $1/\tau_5$, comes from relaxation within $(\alpha, -\alpha)$ pairs. At the lower limit for frequency, $\omega \sim 1/\tau_5$, the range for ξ is limited from above by $\sqrt{\tau_5/\tau}$; see also the Supplemental Material [31].

The magnitude of the anomalous correction to the transmitted field is controlled by the ratio $B_0/B_\alpha(\omega)$ in Eqs. (8)–(10). In the simplified model, there is no dependence on α, and we are able to transform $B_\alpha(\omega) \to B^\star(\omega) = (4/\sqrt{3})B_{\mathrm{uq}}\sqrt{N_W\omega\tau}$. Here B_{uq} is the magnetic field at which the ultra-quantum limit (i.e., only the lowest Landau level is populated) is reached. At the lowest frequencies, $\omega \sim 1/\tau_5$, the characteristic field is $B^\star \sim B_{\mathrm{uq}}\sqrt{N_W\tau/\tau_5}$.

To flesh out the estimates, we use some of the parameters of the Weyl semimetal TaAs [38] derived from Refs. [45,46]: $N_W = 24$, the Fermi velocity $v_F \approx 3 \times 10^7$ cm/s, the Fermi level (measured from a node) $\mu \approx 20$ meV, and the ratio $\tau_5/\tau \approx 158$. We estimate $B_{\mathrm{uq}} \approx 3.5$ T, the upper limit $\xi \sim 13$ for the range of ξ, and the lower limit $B^\star \sim 1.4$ T for $B^\star \sim B_{\mathrm{uq}}\sqrt{N_W\tau/\tau_5}$. The above estimates depend on the ratio τ_5/τ, but not separately on any of these times. To get $\xi \gtrsim 1$, however, one needs $\tau \gtrsim 10$ ps; this is about 25 times higher than the value $\tau \approx 0.38$ ps reported in Refs. [45,46]. One may expect the above quoted ratio τ_5/τ to persist for cleaner samples if both τ and τ_5 are limited by scattering off the same defects. Lastly, at $\tau \sim 10$ ps, fields $B_0 \lesssim 0.02$ T satisfy the condition of a classically weak field.

We illustrate the dependence of the relative field amplitude $|E_{\|\mathrm{out}}|/|E_{\mathrm{out}}(B_0 = 0)| - 1$ on frequency in Fig. 2 for the nonlocal regime. Since cyclotron motion does not affect the conductivity along the direction of a nonquantizing magnetic field ($B_0 \ll B_{\mathrm{uq}}$) for spherical Fermi surfaces [47], we extend the field domain in Eqs. (8)–(10) to $B_0 \lesssim B^\star$. The main qualitative difference between the nonlocal and local regimes is that the chiral anomaly enhances the transmission amplitude in some interval of ω for the former one, while it suppresses the amplitude at any ω in the local regime. Scaling of the transmission amplitude with the film thickness L at $\xi \ll 1$ is controlled by a single parameter $L/\delta(\omega)$; see Eq. (10). In the nonlocal regime, the dependence on L is defined by the normal-skin and diffusion lengths, $\delta(\omega)$ and $\xi\delta(\omega)$, respectively. In certain intervals of L, the anomalous correction competes with the normal-skin term in $E_{\|\mathrm{out}}$ [see Eqs. (8) and (9)], resulting in the negative values of $|E_{\|\mathrm{out}}|/|E_{\mathrm{out}}(B_0 = 0)| - 1$. However, with the raise of frequency, the anomalous term could win over the normal-skin one, as is illustrated by Fig. 2.

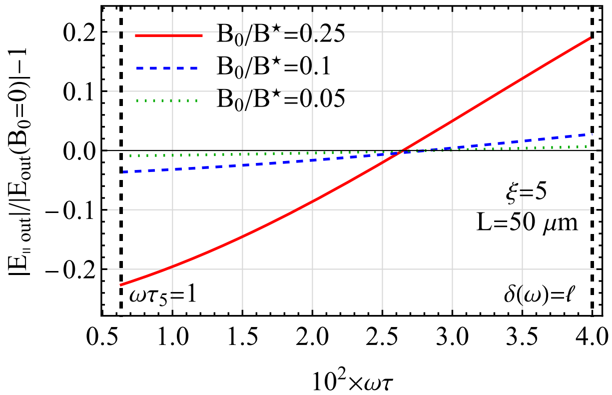

FIG. 2. The dependence of the relative field amplitude $|E_{\|\text{out}}|/|E_{\text{out}}(B_0=0)|-1$ on frequency for a few values of the magnetic field. We used Eq. (9) to plot the results in the nonlocal ($\xi=5$) regime. Black vertical dashed lines are the boundaries of the parameter region where the nonlocal regime under the conditions of the normal-skin effect is realized. We used Neumann boundary conditions and set $B^\star = B_{\text{uq}}\sqrt{N_W\tau/\tau_5}$, $B_{\text{uq}} = c\mu^2/(2e\hbar v_F^2)$, and $L = 50$ μm; other parameters are given in the text.

Discussion and Summary.—We showed that the chiral anomaly may lead to a nonlocal current response of a Weyl or Dirac semimetal even under the conditions of the normal skin effect. The length scale for the nonlocality is determined by the diffusion length of the valley charge imbalance, which does not violate the local electric charge neutrality. This nonlocality is manifested in the penetration and transmission of electromagnetic waves if the diffusion length exceeds the normal-skin depth. Such a regime may be possible in sufficiently clean materials.

The chiral anomaly is activated by a static magnetic field $\mathbf{B}_0$ applied parallel to the surface of the material. The anomaly affects the transmission of an electromagnetic wave with the electric field $\mathbf{E}_\|$ parallel to $\mathbf{B}_0$. In this case, the penetration of the field is sensitive to the competition between the normal and anomalous mechanisms of the electromagnetic field propagation in the material. The penetration of the component of the electric field $\mathbf{E}_\perp$ orthogonal to $\mathbf{B}_0$ is unaffected by the anomaly.

We developed a detailed prediction for the field transmission across the film; see Eqs. (8) and (9) for films thick and thin compared with the diffusion length, respectively, as well as Eq. (10) for the local response regime. In view of a weaker decay of the anomalous components, it might be possible to achieve an enhancement of the electromagnetic wave penetration depth in the nonlocal regime; see Fig. 2. Furthermore, the anomalous part of the transmitted field in the local and nonlocal regimes of the current response is characterized by a different scaling with frequency, cf. Eqs. (8) and (9) with Eq. (10). These features may allow one to identify the nonlocality, even if the electron transport parameters of a sample are not known in advance.

The authors acknowledge useful communications with N. P. Armitage, E. V. Gorbar, and I. A. Shovkovy. This work is supported by NSF Grant No. DMR-2002275 (L. I. G.). P. O. S. acknowledges support through the Yale Prize Postdoctoral Fellowship in Condensed Matter Theory. This work was performed in part at Aspen Center for Physics, which is supported by NSF Grant No. PHY-1607611.

*pavlo.sukhachov@yale.edu

[1] H. Nielsen and M. Ninomiya, The Adler-Bell-Jackiw anomaly and Weyl fermions in a crystal, Phys. Lett. **130B**, 389 (1983).
[2] S. L. Adler, Axial-vector vertex in spinor electrodynamics, Phys. Rev. **177**, 2426 (1969).
[3] J. S. Bell and R. Jackiw, A PCAC puzzle: $\pi_0 \to \gamma\gamma$ in the σ-model, Nuovo Cimento A **60**, 47 (1969).
[4] T. D. C. Bevan, A. J. Manninen, J. B. Cook, J. R. Hook, H. E. Hall, T. Vachaspati, and G. E. Volovik, Momentum creation by vortices in superfluid ^{3}He as a model of primordial baryogenesis, Nature (London) **386**, 689 (1997).
[5] M. Z. Hasan, S.-Y. Xu, I. Belopolski, and S.-M. Huang, Discovery of Weyl fermion semimetals and topological Fermi arc states, Annu. Rev. Condens. Matter Phys. **8**, 289 (2017).
[6] N. P. Armitage, E. J. Mele, and A. Vishwanath, Weyl and Dirac semimetals in three-dimensional solids, Rev. Mod. Phys. **90**, 015001 (2018).
[7] E. V. Gorbar, V. A. Miransky, I. A. Shovkovy, and P. O. Sukhachov, *Electronic Properties of Dirac and Weyl Semimetals* (World Scientific, Singapore, 2021).
[8] D. T. Son and B. Z. Spivak, Chiral anomaly and classical negative magnetoresistance of Weyl metals, Phys. Rev. B **88**, 104412 (2013).
[9] P. Hosur and X. Qi, Recent developments in transport phenomena in Weyl semimetals, C.R. Phys. **14**, 857 (2013).
[10] A. A. Burkov, Chiral anomaly and transport in Weyl metals, J. Phys. Condens. Matter **27**, 113201 (2015).
[11] E. V. Gorbar, V. A. Miransky, I. A. Shovkovy, and P. O. Sukhachov, Anomalous transport properties of Dirac and Weyl semimetals (Review Article), Low Temp. Phys. **44**, 487 (2018).
[12] J. Hu, S.-Y. Xu, N. Ni, and Z. Mao, Transport of Topological Semimetals, Annu. Rev. Mater. Res. **49**, 207 (2019).
[13] N. P. Ong and S. Liang, Experimental signatures of the chiral anomaly in DiracWeyl semimetals, Nat. Rev. Phys. **3**, 394 (2021).
[14] R. D. dos Reis, M. O. Ajeesh, N. Kumar, F. Arnold, C. Shekhar, M. Naumann, M. Schmidt, M. Nicklas, and E. Hassinger, On the search for the chiral anomaly in Weyl semimetals: The negative longitudinal magnetoresistance, New J. Phys. **18**, 085006 (2016).
[15] S. Liang, J. Lin, S. Kushwaha, J. Xing, N. Ni, R. J. Cava, and N. P. Ong, Experimental Tests of the Chiral Anomaly Magnetoresistance in the Dirac-Weyl Semimetals Na_3Bi and GdPtBi, Phys. Rev. X **8**, 031002 (2018).
[16] P. Goswami, J. H. Pixley, and S. Das Sarma, Axial anomaly and longitudinal magnetoresistance of a generic three-dimensional metal, Phys. Rev. B **92**, 075205 (2015).

[17] A. A. Burkov, Dynamical density response and optical conductivity in topological metals, Phys. Rev. B **98**, 165123 (2018).

[18] B. Cheng, T. Schumann, S. Stemmer, and N. P. Armitage, Probing charge pumping and relaxation of the chiral anomaly in a Dirac semimetal, Sci. Adv. **7**, eabg0914 (2021).

[19] A. A. Abrikosov, *Fundamentals of the Theory of Metals* (Courier Dover Publications, New York, 2017).

[20] A. Vilenkin, Equilibrium parity-violating current in a magnetic field, Phys. Rev. D **22**, 3080 (1980).

[21] K. Fukushima, D. E. Kharzeev, and H. J. Warringa, Chiral magnetic effect, Phys. Rev. D **78**, 074033 (2008).

[22] S. A. Parameswaran, T. Grover, D. A. Abanin, D. A. Pesin, and A. Vishwanath, Probing the Chiral Anomaly with Nonlocal Transport in Three-Dimensional Topological Semimetals, Phys. Rev. X **4**, 031035 (2014).

[23] C. Zhang, E. Zhang, W. Wang, Y. Liu, Z.-G. Chen, S. Lu, S. Liang, J. Cao, X. Yuan, L. Tang, Q. Li, C. Zhou, T. Gu, Y. Wu, J. Zou, and F. Xiu, Room-temperature chiral charge pumping in Dirac semimetals, Nat. Commun. **8**, 13741 (2017).

[24] J. C. de Boer, D. H. Wielens, J. A. Voerman, B. de Ronde, Y. Huang, M. S. Golden, C. Li, and A. Brinkman, Nonlocal signatures of the chiral magnetic effect in the Dirac semimetal $Bi_{0.97}Sb_{0.03}$, Phys. Rev. B **99**, 085124 (2019).

[25] The main qualitative results of our study should hold for a time-reversal symmetry broken Weyl semimetal as well. However, such systems have other phenomena that also affect the propagation and reflection of electromagnetic waves, *e.g.*, anomalous Kerr and Faraday effects [26]. These phenomena are ignored in this work where we focus on the effects of the chiral anomaly.

[26] M. Kargarian, M. Randeria, and N. Trivedi, Theory of Kerr and Faraday rotations and linear dichroism in Topological Weyl Semimetals, Sci. Rep. **5**, 12683 (2015).

[27] M. M. Jadidi, M. Kargarian, M. Mittendorff, Y. Aytac, B. Shen, J. C. König-Otto, S. Winnerl, N. Ni, A. L. Gaeta, T. E. Murphy, and H. D. Drew, Nonlinear optical control of chiral charge pumping in a topological Weyl semimetal, Phys. Rev. B **102**, 245123 (2020).

[28] The cyclotron frequency for the classically-weak magnetic field is smaller than the intra-node scattering rate, *i.e.*, $\omega_c \ll \min\{1/\tau_{\alpha,\alpha}\}$, where $1/\tau_{\alpha,\alpha}$ is the intra-node scattering rate for Weyl node α.

[29] We disregard the contribution of the Fermi arc surface states in the current. As is estimated in Ref. [30], the relative contribution of the Fermi arcs to the surface impedance is negligible if the frequency of the impinging wave is much smaller than the plasmon resonance frequency, which is indeed the case in our study.

[30] Q. Chen, A. R. Kutayiah, I. Oladyshkin, M. Tokman, and A. Belyanin, Optical properties and electromagnetic modes of Weyl semimetals, Phys. Rev. B **99**, 075137 (2019).

[31] See Supplemental Material at http://link.aps.org/supplemental/10.1103/PhysRevLett.128.146801 for the derivations of the kinetic equations and the transmission of electromagnetic waves in the nonlocal and local current response regimes. The Supplemental Material contains Refs. [32–35].

[32] D. Xiao, M. C. Chang, and Q. Niu, Berry phase effects on electronic properties, Rev. Mod. Phys. **82**, 1959 (2010).

[33] D. T. Son and N. Yamamoto, Kinetic theory with Berry curvature from quantum field theories, Phys. Rev. D **87**, 085016 (2013).

[34] M. A. Stephanov and Y. Yin, Chiral Kinetic Theory, Phys. Rev. Lett. **109**, 162001 (2012).

[35] L. D. Landau, E. M. Lifshits, and L. P. Pitaevskii, *Electrodynamics of Continuous Media* (Butterworth-Heinemann, Oxford, 1984).

[36] A. A. Burkov, Chiral Anomaly and Diffusive Magnetotransport in Weyl Metals, Phys. Rev. Lett. **113**, 247203 (2014).

[37] The continuity of the derivatives of the tangential components of electric fields at the surfaces follows from the continuity of the tangential components of the magnetic fields.

[38] While we use the parameters of the Weyl semimetal TaAs, other materials with a simpler band structure might be used to observe the proposed anomalous nonlocal effect. For example, we mention the Dirac semimetal Cd_3As_2 [39–41] and the Weyl semimetal $EuCd_2As_2$ [42–44]. Compared to TaAs, they have a simpler band structure with only two Dirac points and Weyl nodes, respectively.

[39] S. Borisenko, Q. Gibson, D. Evtushinsky, V. Zabolotnyy, B. Büchner, and R. J. Cava, Experimental Realization of a Three-Dimensional Dirac Semimetal, Phys. Rev. Lett. **113**, 027603 (2014).

[40] Z. K. Liu, J. Jiang, B. Zhou, Z. J. Wang, Y. Zhang, H. M. Weng, D. Prabhakaran, S.-K. Mo, H. Peng, P. Dudin, T. Kim, M. Hoesch, Z. Fang, X. Dai, Z. X. Shen, D. L. Feng, Z. Hussain, and Y. L. Chen, A stable three-dimensional topological Dirac semimetal Cd_3As_2, Nat. Mater. **13**, 677 (2014).

[41] M. Neupane, S.-Y. Xu, R. Sankar, N. Alidoust, G. Bian, C. Liu, I. Belopolski, T.-R. Chang, H.-T. Jeng, H. Lin, A. Bansil, F. Chou, and M. Z. Hasan, Observation of a three-dimensional topological Dirac semimetal phase in high-mobility Cd_3As_2, Nat. Commun. **5**, 3786 (2014).

[42] L.-L. Wang, N. H. Jo, B. Kuthanazhi, Y. Wu, R. J. McQueeney, A. Kaminski, and P. C. Canfield, Single pair of Weyl fermions in the half-metallic semimetal $EuCd_2As_2$, Phys. Rev. B **99**, 245147 (2019).

[43] J.-R. Soh, F. de Juan, M. G. Vergniory, N. B. M. Schröter, M. C. Rahn, D. Y. Yan, J. Jiang, M. Bristow, P. A. Reiss, J. N. Blandy, Y. F. Guo, Y. G. Shi, T. K. Kim, A. McCollam, S. H. Simon, Y. Chen, A. I. Coldea, and A. T. Boothroyd, Ideal Weyl semimetal induced by magnetic exchange, Phys. Rev. B **100**, 201102(R) (2019).

[44] J.-Z. Ma, S. M. Nie, C. J. Yi, J. Jandke, T. Shang, M. Y. Yao, M. Naamneh, L. Q. Yan, Y. Sun, A. Chikina, V. N. Strocov, M. Medarde, M. Song, Y.-M. Xiong, G. Xu, W. Wulfhekel, J. Mesot, M. Reticcioli, C. Franchini, C. Mudry, M. Müller, Y. G. Shi, T. Qian, H. Ding, and M. Shi, Spin fluctuation induced Weyl semimetal state in the paramagnetic phase of $EuCd_2As_2$, Sci. Adv. **5**, eaaw4718 (2019).

[45] F. Arnold, M. Naumann, S.-C. Wu, Y. Sun, M. Schmidt, H. Borrmann, C. Felser, B. Yan, and E. Hassinger, Chiral Weyl Pockets and Fermi Surface Topology of the Weyl Semimetal TaAs, Phys. Rev. Lett. **117**, 146401 (2016).

[46] C.-L. Zhang, S.-Y. Xu, I. Belopolski, Z. Yuan, Z. Lin, B. Tong, G. Bian, N. Alidoust, C.-C. Lee, S.-M. Huang, T.-R. Chang, G. Chang, C.-H. Hsu, H.-T. Jeng, M. Neupane, D. S. Sanchez, H. Zheng, J. Wang, H. Lin, C. Zhang, H.-Z. Lu, S.-Q. Shen, T. Neupert, M. Zahid Hasan, and S. Jia, Signatures of the AdlerBellJackiw chiral anomaly in a Weyl fermion semimetal, Nat. Commun. **7**, 10735 (2016).

[47] I. M. Lifshitz, M. I. Azbel, and M. I. Kaganov, The theory of galvanomagnetic effects in metals, J. Exp. Theor. Phys. **4**, 41 (1957), http://www.jetp.ras.ru/cgi-bin/e/index/e/4/1/p41?a=list.